Dalton Transactions

Accepted Manuscript

This article can be cited before page numbers have been issued, to do this please use: G. A. M. Ali, D. Aravind, S. S, K. F. Chong, A. Ethiraj, M.V Reddy, H. Gharni and G. Hegde, *Dalton Trans.*, 2017, DOI: 10.1039/C7DT02392H.

This is an Accepted Manuscript, which has been through the Royal Society of Chemistry peer review process and has been accepted for publication.

Accepted Manuscripts are published online shortly after acceptance, before technical editing, formatting and proof reading. Using this free service, authors can make their results available to the community, in citable form, before we publish the edited article. We will replace this Accepted Manuscript with the edited and formatted Advance Article as soon as it is available.

You can find more information about Accepted Manuscripts in the author guidelines.

Please note that technical editing may introduce minor changes to the text and/or graphics, which may alter content. The journal's standard Terms & Conditions and the ethical guidelines, outlined in our author and reviewer resource centre, still apply. In no event shall the Royal Society of Chemistry be held responsible for any errors or omissions in this Accepted Manuscript or any consequences arising from the use of any information it contains.

ROYAL SOCIETY OF CHEMISTRY

rsc.li/dalton

View Article Online
DOI: 10.1039/C7DT02392H

Dalton Transactions

ARTICLE

Carbon nanospheres derived from Lablab Purpureus as a high performance supercapacitor electrode: Green approach†

Received 00th January 20xx,
Accepted 00th January 20xx

DOI: 10.1039/x0xx00000x

www.rsc.org/

Gomaa A. M. Ali[ab1], Divyashree A[c1], Supriya S[c], Kwok Feng Chong[a], Anita S. Ethiraj[d], M V Reddy[e], H. Algarni[f] and Gurumurthy Hegde[c*]

Carbon nanospheres derived from natural source using a green approach were reported. Lablab Purpureus seeds were pyrolyzed at different temperatures, to produce carbon nanospheres for supercapacitor electrode materials. The synthesized carbon nanospheres were analyzed using SEM, TEM, FTIR, TGA, Raman Spectroscopy, BET and XRD. They were later fabricated into electrodes for cyclic voltammetry, galvanostatic charge/discharge and electrochemical impedance spectroscopy testings. The specific capacitances were found to be 300, 265 and 175 F g^{-1} in 5 M KOH electrolyte for carbon nanospheres synthesized at 800, 700 and 500 ^{o}C, respectively. These are at par with prior electrodes made of biologically derived carbon nanospheres but the cycles life were remarkably higher than any previous efforts. The electrodes showed 94% capacitance retention even after 5200 charge/discharge cycles entailing excellent recycling durability. In addition, the practical symmetrical supercapacitor showed a good electrochemical behaviour under potentials window up to 1.7 V. This brings us one step closer to fabricating a commercially green electrode which exhibits high performance for supercapacitors. This is also a waste to wealth approach based carbon materials for cost effective supercapacitors with high performance for power storage devices.

1. Introduction

Batteries use electrochemical reactions to store and produce electricity [1]. In a lithium ion battery, the lithium ions move between the electrodes to produce electricity [2]. In a rechargeable battery, a reverse potential helps move the ions back into their original position [3]. The electrochemical process is slow and over the time degrades the electrodes. This limits the usable life to a few thousand charge/discharge cycles leading to a short life in turn leading to the issue of disposal [4]. The popular Li–Ion and Ni–Cd batteries contain highly toxic chemicals [5, 6] and they must be disposed by in a controlled environment. In developing country like India and China where regulations are difficult to be enforced, the unregulated disposal often lead to an environmental crisis where expensive ground cleaning operations are often needed [7].

Unlike batteries, supercapacitors store energy in an electric field [8], and no movement of ions to degrade its performance. They can be charged/discharged rapidly and have millions of cycles before the performance begins to degrade [9]. Supercapacitors traditionally suffer from a lower energy density when compared to batteries [10]. The supercapacitors electrode materials can be classified into three main categories based on the charge storage mechanism (carbon–based materials [11-15], transition metal oxides [16-21] and hybrid materials [22-25]). If there was an order of magnitude increase in energy storage capability, they will be an ideal replacement for batteries.

Over billions of years of evolution, nature has succeeded in building an ecosystem that can be recycled completely. Every natural product has a predictable lifecycle from birth to death before it is merged back into nature. If the energy storage devices are made by using biological materials, we could have recyclable batteries with long lives and least toxicity. The natural lignocellulosic components are gaining immense attention in energy storage application because of their easy availability, low cost and their low toxicity [26]. The studies as on date, suggests that there are chiliad varieties of plants that

[a] Faculty of Industrial Sciences & Technology, Universiti Malaysia Pahang, Gambang, 26300, Kuantan, Malaysia.
[b] Chemistry Department, Faculty of Science, Al–Azhar University, Assiut, 71524, Egypt
[c] Centre for Nano-Materials and Displays, BMS R&D Centre, BMS College of Engineering, Bull Temple Road, Bangalore, 560019, India
[d] Centre for Nanotechnology Research, VIT University, Vellore, 632014, Tamil Nadu, India
[e] Department of Materials Science and Engineering, National University of Singapore, 9 Engineering Drive 1, 117575, Singapore
[f] Research Center for Advanced Materials Science (RCAMS), King Khalid University, Abha 61413, P. O. Box 9004, Saudi Arabia.
* Corresponding author E-mail address: murthyhegde@gmail.com
[1] Contributed equally to the manuscript as the first author
† Electronic Supplementary Information (ESI) available: [details of any supplementary information available should be included here]. See DOI: 10.1039/x0xx00000x

View Article Online
DOI: 10.1039/C7DT02392H

could be made use of in obtaining nanoparticles for use in energy storage devices [27, 28]. Most common form of nanoparticle that can be produced from a wide variety of plants is carbon nanospheres.

Carbon nanospheres have a spherical shape and inherently possess porosity which is the main characteristic required in energy storage application [29]. They are produced by heating carbon precursors under a controlled atmosphere. The sphere size depends on several factors such as the starting material, the reactor conditions, ground particle size etc. Carbon nanospheres can be produced from many raw materials. These raw materials are expected to be easily available, cost effective and environmentally safe for its use as a precursor in the production (catalyst free process) of carbon nanospheres [30].

Any material having a high composition of carbon and low inorganic content can used as a fore–runner in the production of carbon nanospheres [31]. Subsequently all lignocellulosic materials can be used as a predecessor for the preparation of carbon nanospheres [32] but only a few materials are really good in producing uniform shapes. The use of agro based by–products in carbon nanospheres production is found to be renewable and relatively less expensive in the current trend [30].

In this paper, the energy storage capabilities and performance of electrodes made using a popular legume, *Lablab Purpureus* seeds will be studied. Waste to wealth based approach is adopted in this manuscript to show the ability of bulk production for such kind of materials.

2. Experimental procedures

2.1 Samples preparation

Lablab Purpureus seeds were collected and dried in an oven at a temperature of 100 ˚C for overnight to annihilate all the moisture content in the biowaste precursor. The dried *Lablab Purpureus* (LP) seeds were ground to a fine powder using a grinder (Retsch, ZM 200, Germany) at a speed of 12,000 rpm. The fine powder obtained after grinding was sieved to obtain a uniform particle size of 60 µm. The finely ground uniform sample obtained after sieving was individually pyrolysed under nitrogen (N_2) atmosphere (at a flow rate of 150 mL/cm^3) at different temperatures of 500, 700 and 800 ^oC respectively at a heating rate of 10 ^oC/min using a quartz tube furnace (Figure S1) (NoPo Nanotechnologies, TZ4L Temperature controller, India). The template approach where porosity comes from natural ligno cellulosic materials was incorporated in order to eliminate the silica from the pyrolysed samples and to obtain pure carbon nanospheres. The samples were washed using 2.5 M NaOH solution followed by washing with double deionized water. The detailed study on the preparation of carbon nanospheres is reported in our previous work [33, 34].

2.2 Samples characterization

The raw sample was characterized using Thermo Gravimetric Analysis (TGA) (SDT Q600 V20.9 Build 20). The morphology of the carbon nanospheres obtained after pyrolysis (LP500, LP700 and LP800) was characterized using Field Emission Scanning Electron Microscope–Energy Dispersive X–ray. (SEM–EDX) (JEOL, JSM–7800F) and Transmission Electron Microscope (TEM) (JEOL, JSM–1230). The surface area of the carbon nanospheres was calculated by Brunauer–Emmett–Teller (BET) method of N_2 adsorption data making use of Micromeritics ASAP 2020. The products were degassed for 12 hours at a temperature of 200 ^oC before the measurements. X–ray Diffraction (XRD) patterns were recorded using X–ray diffractometer (RigakuMineflex II), Raman spectrum of the obtained products was recorded using EnWave Optronics ProRaman 532 nm. Fourier Transform Infrared Spectroscopy (FTIR) (Perkin, Elmer Spectrum 100).

2.3 Fabrication of electrode and electrochemical studies

The working electrode was prepared by coating homogenous mixture of carbon nanospheres, carbon black and PVDF in the ratio of 90:5:5 in NMP onto nickel foam. A platinum wire was used as a counter electrode and Ag/AgCl was used as a reference electrode. All the electrochemical experiments were conducted in KOH electrolyte (1.0, 2.5 and 5.0 M). The data were collected using an electrochemical workstation (Autolab/PGSTAT M101) equipped with a frequency response analyser. Cyclic voltammetry tests were performed between -1 and 0 volt with scan rates ranging from 5 to 100 mV s^{-1}. Galvanostatic charge/discharge tests were performed at current densities ranging from 0.1 to 1.0 A g^{-1}. Impedance data were collected from 500 kHz to 0.01 Hz, with 10 mV in an alternating current amplitude signal at open circuit potential (OCP). A practical symmetrical supercapacitor has been made using two electrodes of the active material electrically isolated from each other by porous membrane pre–soaked with the electrolyte solution. It was then sandwiched and pressed into a coin cell design.

3. Results and discussion

3.1 Structural and morphological characterizations

Thermo Gravimetric Analysis (TGA) is used to comprehend the thermal stability of a material before deciding its pyrolysis temperature. The TG curve of the raw *Lablab Purpureus* seeds heated from room temperature to 1200 ^oC in N_2 atmosphere (Figure S2). It is evident that the thermal degradation takes place in three steps. At the first stage, it is seen that there is a weight loss of ~8% at a temperature less than 150 ^oC. This weight loss in the precursor can be attributed to the water molecules desorption from the surface of the precursor. At the second stage, a weight loss of roughly about ~61% is encountered in the temperature range of 150–390 ^oC, which is

View Article Online
DOI: 10.1039/C7DT02392H
Dalton Transactions ARTICLE

due to the thermal degradation of plant residues in the precursor. The thermal degradation of the material ends at a temperature of ~400 ^{o}C, therefore any temperature higher than 400 ^{o}C can be considered to synthesize carbon nanospheres from the precursor. Henceforth, we can observe a gradual weight loss in the precursor up to a temperature of 1200 ^{o}C and in the whole process, we observe no weight gain in the precursor inferring that the precursor remained intact due to the N_2 atmosphere [35].

The morphology of *Lablab Purpureus* seeds and the mass ratios the elements present in the raw seeds were studied using SEM combined with EDX. Figure S3(a) shows the morphology and Figure S3(b) shows the EDX spectrum (inset: mass ratios of the elements) of *Lablab Purpureus* seeds before pyrolysis. The EDX spectrum validates the presence of a rich amount of carbon content (61.1 wt.%) in comparison with oxygen (36.6 wt.%) along with small percentage of other elements like Mg : 0.54 wt%, Cl : 0.45 wt%, K :0.86 wt% and Ca : 0.33 wt%. in the precursor.

Fourier Transform Infrared (FTIR) analysis is used to study the functional group present in the sample. FTIR spectrum shows the active bonds in *Lablab Purpureus* seeds which attribute to the formation of carbon nanomaterials after pyrolysis (Figure S4). The broad band at 3432 cm^{-1} represents the hydrogen bonded –O–H stretching vibration of α–cellulose and also confirms the presence of compounds with alcoholic groups like polyphenols and flavonoids [36]. The bands at 2926 cm^{-1} and 2864 cm^{-1} show C–H stretching of lignocellulosic components [37]. The band observed at 1649 cm^{-1} represents C=O stretching vibration in conjugated carbonyl of lignin. The band at 1418 cm^{-1} show the aromatic skeletal combined with C–H in plane deforming and stretching in lignin and the band at 1028 cm^{-1} is due to the C–O vibrational stretching of primary alcohols [38]. Thus, FTIR analysis of *Lablab Purpureus* seeds affirms the presence of cellulose, hemicellulose and lignin. The raw Lablab Purpureus seeds were pyrolysed at three different temperatures (500, 700 and 800 ^{o}C) in a quartz tube furnace under a continuous flow of N_2. In order to eliminate the ash, the pyrolysed products (coded as: LP500, LP700 and LP800) were washed separately using 0.1 M HCl solution and then followed by double distilled water. The detailed description of carbon nanospheres synthesis is described in our earlier work [39]. The total yield of carbon nanospheres obtained after pyrolysis of Lablab Purpureus seeds at three different temperatures was approximate 22%.

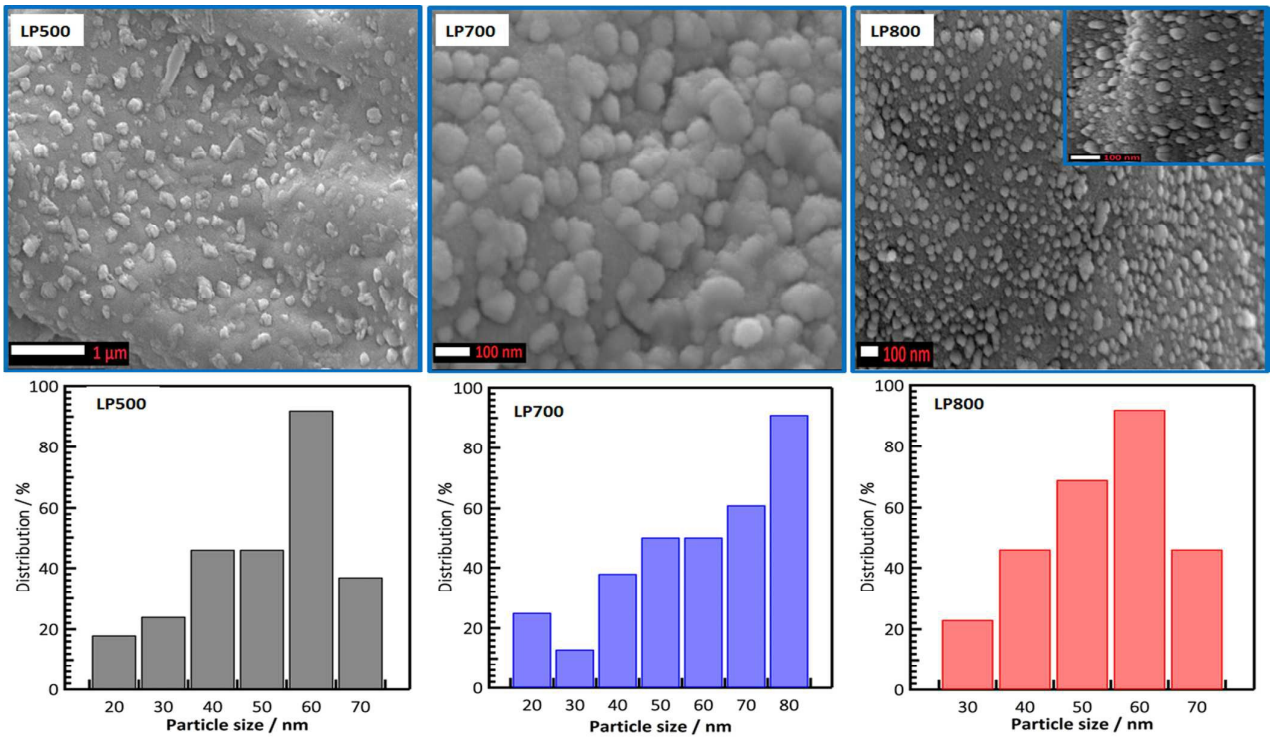

Figure 1 SEM images and particle size distribution histograms of the indicated materials.

View Article Online
DOI: 10.1039/C7DT02392H

The structure, shape and the mass ratios of the elemental composition of the materials obtained after pyrolysis were examined with the help of SEM/EDX and TEM analysis. Figure 1 shows the SEM images and particles size distribution histograms of the carbon nanospheres synthesized at 500, 700 and 800 °C (LP500, LP700 and LP800). From Figure 1, it is noticeable that the carbon nanospheres derived from *Lablab Purpureus* seeds are all vaguely uniform and spherical in shape. The LP500 synthesized at 500 °C has a particle size ranging between 40–60 nm (a and b), the LP700 synthesized at 700 °C has a particle size in the range of 70–80 nm (c and d) and the LP800 synthesized at 800 °C has a uniform distribution and a particle size in the range of 50–60 nm which is evident from the inset and the histograms. As temperature increases, it might go towards graphitic nature of the particle which definitely reduces the size of the nanoparticles, which is evident from various other works. Higher the temperature can lead to smaller particle size or larger surface area.

Table S1 shows the elemental composition of the carbon nanospheres synthesized from *Lablab Purpureus* seeds at different temperatures (500, 700 and 800 °C). The elemental analysis asserts the presence of elements like carbon, oxygen and potassium in considerable percentage. EDX measurements reveal that the spheres consist predominantly of carbon. From Table S1, it is evident that the percentage of carbon has increased with the increase in the pyrolysis temperature.

The transmission electron microscopy (TEM) for the carbon nanospheres synthesized from *Lablab Purpureus* seeds gave the regular pore image at carbonization temperatures of 500, 700 and 800 °C, where the average particle size is 85±5 nm (Figure S5(a)), 80±5 nm (Figure S5(c)) and 90±5 nm (Figure S5(e)) and their corresponding mounting images (Figure S5(b), (d) and (f), respectively). TEM images suggest the porous structure present in them.

The surface properties of the carbon nanospheres derived from *Lablab Purpureus* seeds synthesized at 800 °C (LP800) was investigated using N_2 adsorption and desorption to obtain the pore size, and Brunauer–Emmett–Teller (BET) surface area. The carbon nanospheres obtained at 800 °C (LP800) is used because of its uniform shape and smaller size unlike LP500 and LP700. The N_2 adsorption and desorption curves of LP800 are as shown in Figure 2. The BET surface area of LP800 was found to be 42.2 $m^2 g^{-1}$ with pore volume of 0.033 cm^3/g and pore width of 3.13 nm. The pore diameter calculated from the graph was found to be 2-3 nm. The obtained BET surface area of LP800 is relatively less in comparison to other reported spherical carbon nanoparticles [40, 41], but comparable to carbon nanospheres synthesized from biowaste lignocellulosic materials [33]. The low surface area of the carbon nanospheres may be due to the particles agglomeration.

A comparative powder XRD diffractograms of the LP500, LP700 and LP800 synthesized from *Lablab Purpureus* seeds at different temperatures (500, 700 and 800 °C) is as shown in Figure 3. The peaks observed at 2θ = ~29.8° and 2θ = ~40.5° can be assigned to graphitic (0 2 0) and (0 0 2) planes (ICDD no. 96–901–2234). The peak which is encountered at 2θ = ~28° can be attributed to (1 1 0) plane (ICDD no. 96–901–2238) of crystalline cellulose fibres which are created due to the presence of hemicellulose and cellulose in *Lablab Purpureus* seeds [42]. The peak witnessed at 2θ = ~41° denotes the hexagonal graphite lattice present in the carbon nanospheres [43]. From the diffractogram it is clear that the carbon nanospheres synthesized at a higher temperature is more graphitic in nature.

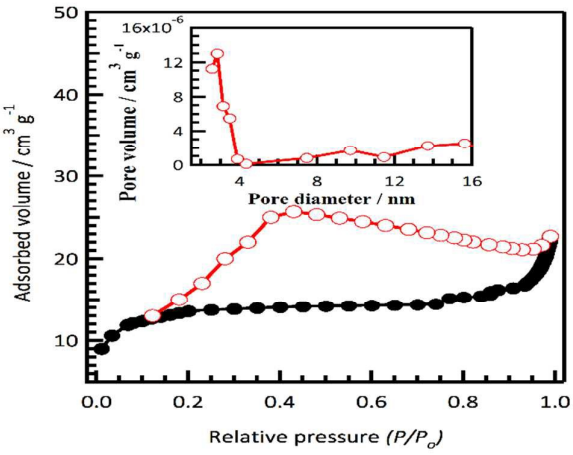

Figure 2 N_2 adsorption and desorption curves; the inset shows the pore size distribution of LP800.

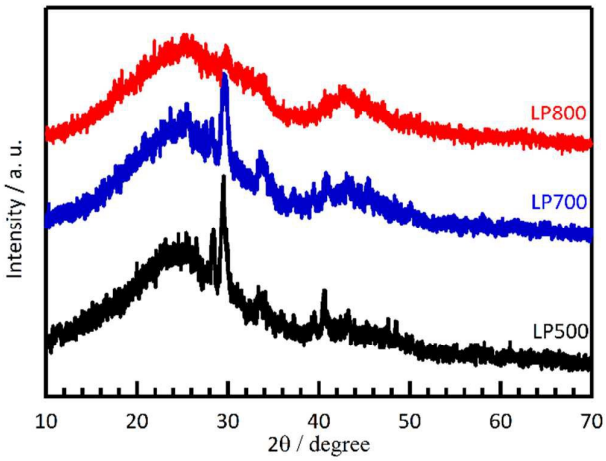

Figure 3 XRD diffractograms of the indicated materials.

The degree of graphitization and the lattice vibration of the carbon nanopsheres were studied using Raman spectroscopy. Raman spectra of LP500, LP700 and LP800 show least difference in the position of D and G band in all the samples (Figure S6). The occurrence of D and G bands is majorly due to the defects and disorder present in the graphitic structure. The prevalence of the D–band here at ~1461 cm^{-1} attributed to the

View Article Online
DOI: 10.1039/C7DT02392H

disordered structure of carbon nanospheres and also to the A_{1g} mode. This band also authenticates the presence of structural defects and disorders in carbon nanospheres [44]. The sharp D–band which is as seen in the spectrum indicates that the bonds are very uniform in nature. The G–band which is positioned at ~1524 cm^{-1} is due to the E_{2g} model at the Γ–point. It is produced due to the stretching of the C=C bond in the graphitic materials and is common to all the sp^2–bonded carbon systems [45]. The relative intensity ratio (I_D/I_G) of these bands reveals the graphitic characteristics. I_D/I_G of the carbon nanospheres (LP500, LP700 and LP800) was found to be ~0.95. This signifies the turbostatic structure of the parallel graphene sheets [46].

During pyrolysis, the carbon precursor *Lablab Purpureus* seeds undergo decomposition; the functional groups are majorly lost in the process forming only the carbon. However, traces of functional groups which were previously present in the raw materials are observed in carbonized material and can be explained by their FITR spectra (Figure S7). The broad band at 3438 cm^{-1} can be attributed to stretching of O–H in traces of alcoholic compounds and also represents any moisture content present in the resulted material. C–H stretching vibrations of any alkyl group result in the band at 2909 cm^{-1} [37]. The band at 1622 cm^{-1} may represent the formation of the C=C bond during pyrolysis; this even indicates that the material formed has obtained graphitic nature. The presence of any aromatic molecule in the carbonized material can be indicated by the band at 1404 cm^{-1} which is due to bending of $=CH_2$ in the aromatic ring. The small band at 1017 cm^{-1} may indicate C–O stretching in alcoholic groups [38]. From the spectrum of pyrolysed material, it can be said that seeds of *Lablab Purpureus* result in the formation of a carbonaceous material with graphitic nature, which is an important property that makes it desirable in energy storage applications.

3.2 Electrochemical studies

3.2.1 Supercapacitor electrodes performance

The electrochemical behavior and the stability of the electrodes fabricated from carbon nanospheres synthesized from *Lablab Purpureus* seeds were studied using galvanostatic charge/discharge cycling and cyclic voltammetry (CV) tests. The electrochemical performances of the electrodes were studied in 5.0 M KOH solution after initial stabilization for 20 CV cycles at a scan rate ranging between of 5 to 100 mV s^{-1} in a potential window of -1–0 V.

3.2.1.1 Effect of electrolyte concentration

CV studies were made on carbon nanospheres at different scan rates ranging from 5 to 100 mV s^{-1} which is as shown in Figure 4. A quasi rectangular shaped CV curve is obtained in the case of LP700 and LP800 but the CV curve of LP500 is smaller in comparison with LP700 and LP800. There are no significant redox peaks in the CV curves of all the three samples which emboss the behaviour of an ideal ELDC [47]. From Figure 4, it is conspicuous that the shape of the CV curves slightly differs from the shape of the CV curve of an ideal supercapacitor which can be attributed to various factors like; temperature of synthesis, electrolyte and its concentration, fabrication methods etc. From Figure 4(a, b, c), it is evident that the performance of the electrode fabricated from the precursor synthesized at 800 °C (LP800) is better in comparison with the electrode fabricated from the precursor synthesized at 700 and 500 °C, demonstrating superior ion transportation at a high charge and discharge rate and manifesting ideal capacitive behaviour.

Furthermore, the galvanostatic charge/discharge curves of the carbon nanospheres synthesized from *Lablab Purpureus* seeds at different temperatures authenticates that all the curves are eminently linear and symmetrical (Figure 5) at a current density of 0.5 A g^{-1} and at different electrolyte concentration (1.0, 2.5 and 5 M KOH). This signifies that the carbon nanospheres synthesized from *Lablab Purpureus* seeds have eminent electrochemical reversibility and charge/discharge property. It is also distinct that *iR* (voltage) drops for all the curves are negligible even at 0.5 A g^{-1}, clearly indicating very bleak overall resistance and pronounced capacitive properties. From Figure 5 it is evident that the carbon nanospheres synthesized at 800 °C in 5 M KOH electrolyte concentration shows excellent results in comparison with the carbon nanospheres synthesized at 500 and 700 °C in 1.0 and 2.5 M KOH electrolyte concentrations. The specific capacitance of the electrodes from all the three samples from charge/discharge data was calculated using the equation reported elsewhere [48, 49]. The specific capacitances were found to be 300, 260 and 174 F g^{-1} respectively for LP800, LP700 and LP500 in 5 M KOH electrolyte. A comparison study with other carbon based materials in view of specific capacitance is shown in Table 1.

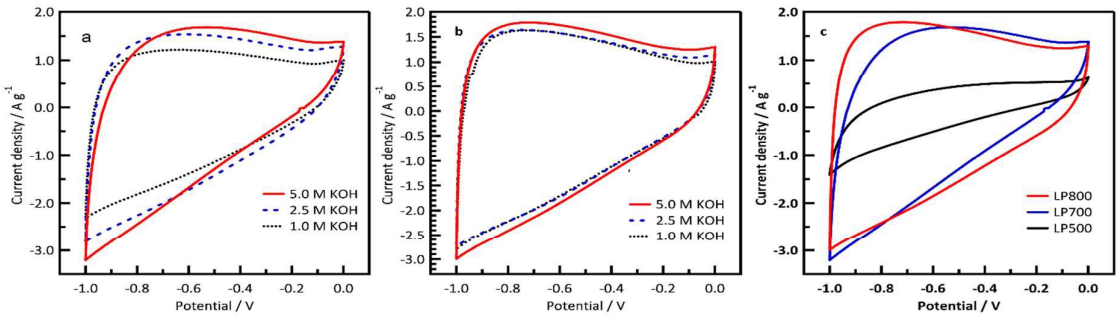

Figure 4 Cyclic voltammetry curves at a scan rate of 25 mV s^{-1} in different electrolyte concentrations for LP700 (a), LP800 (b) and comparative CV curves of all materials (c) in 5 M KOH.

View Article Online
DOI: 10.1039/C7DT02392H

Dalton Transactions

ARTICLE

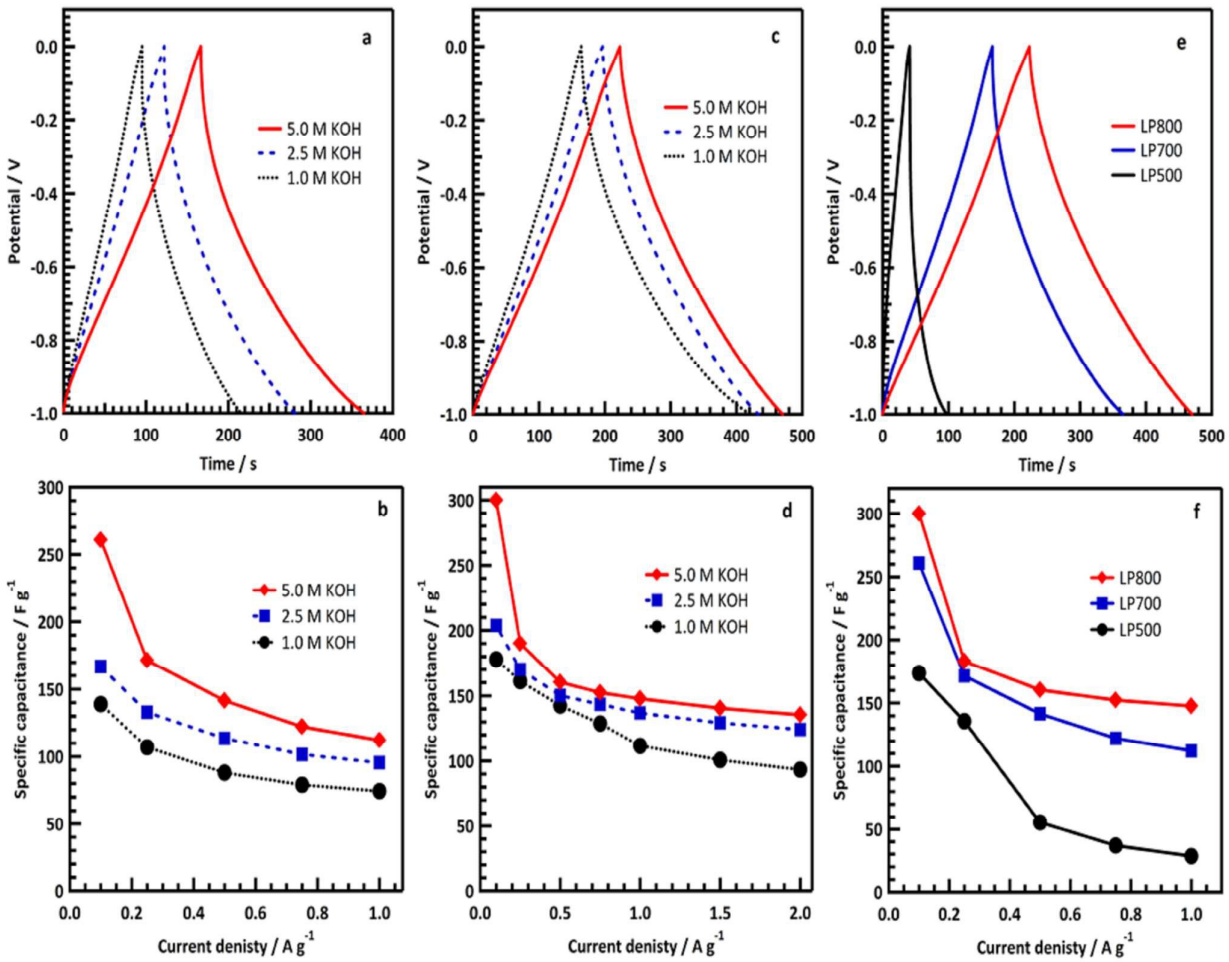

Figure 5 Galvanostatic charge/discharge curves at 0.5 A g^{-1} and specific capacitance as a function of current density in different electrolyte concentrations for LP700 (a, b), LP800 (c, a) and comparison of LP500, LP700 and LP800 (e, f) in 5 M KOH.

3.2.1.2 Effect of carbonization temperature

The concomitant of pyrolysis temperature on the electrochemical properties of the carbon nanospheres derived from *Lablab Purpureus* seeds was studied using cyclic voltammetry and galvanostatic charge–discharge in 5 M KOH electrolyte concentration (Figure 6). Cyclic voltammetry curves of the carbon nanospheres synthesized at different temperatures (500, 700 and 800 ^{o}C) at different scan rates (10, 25, 50, 75 and 100 mV s^{-1}) are shown in Figure 6(a–c). It is evident from Figure 6, that the carbon nanospheres synthesized at 800 ^{o}C (LP800) is better in comparison with the other samples (LP500 and LP700). The galvanostatic charge/discharge curves of the carbon nanospheres (LP500, LP700 and LP800) at different current densities (Figure 6(d–f)) show that the discharge capacitance increased with the increase in synthesis temperature at all current densities. The charge/discharge curves are nearly linear and the ion discharge time gingerly increases with the increase in carbonization temperature.

View Article Online
DOI: 10.1039/C7DT02392H
Dalton Transactions ARTICLE

Table 1 Comparison of reported specific capacitance with carbon based materials.

Material	Specific capacitance (F g^{-1})	Ref.
Activated carbon derived from banana fibers	74 @ 0.5 A g^{-1}	50
Sugar–derived carbon/graphene composite	273 @ 0.5 A g^{-1}	51
KOH–treated commercial activated carbon	200 @ 0.05 A g^{-1}	52
Melamine–based carbon	204.8 @ 0.02 A g^{-1}	53
Activated carbons from Argania spinosa seed shells	259 @ 0.125 A g^{-1}	54
Novel corn grains–based activated carbons	257 @ 0.1 A g^{-1}	55
Electrochemically reduced graphene nanosheets	131 @ 0.1 A g^{-1}	56
Hydrazine reduced graphene nanosheets	140 @ 0.05 A g^{-1}	12
Activated carbons from waste Camellia oleifera shell	266 @ 0.2 A g^{-1}	57
Porous nanocarbons from biowaste oil palm leaves	368 @ 0.06 A g^{-1}	34
Carbon nanospheres from *Lablab Purpureus seeds*	*300 @ 0.1* A g^{-1}	*This work*

View Article Online
DOI: 10.1039/C7DT02392H

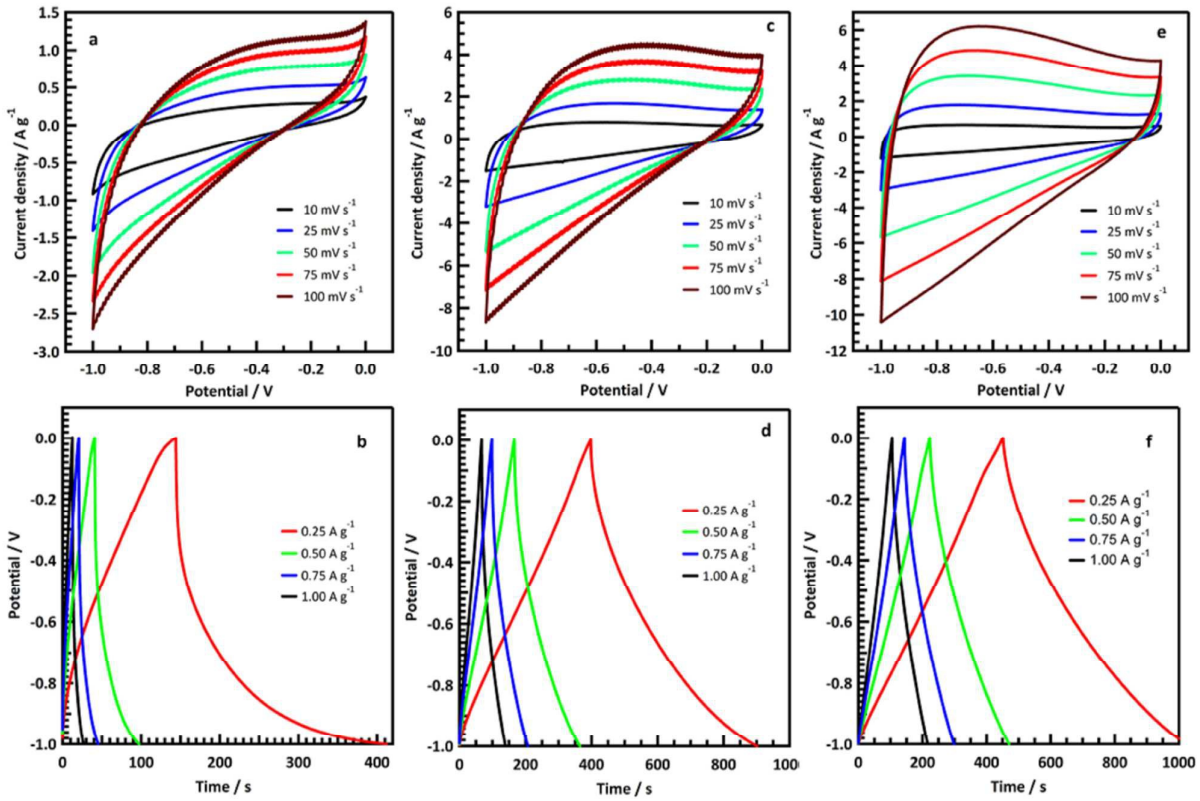

Figure 6 Cyclic voltammetry at different scan rates and galvanostatic charge/discharge curves at different current densities for LP500 (a, b), LP700 (c, d) and LP800 (e, f).

3.2.1.3 Cycle life stability

To affirm the potential liability of carbon nanospheres derived from *Lablab Purpureus* seeds in supercapacitor application, the cyclic stability of the electrode was analysed by charge/discharge cycle testing.

The stability of the carbon nanospheres was studied using galvanostatic charge/discharge at a current density of 3 A g^{-1} for 5,200 cycles and presented in Figure 7. The carbon nanospheres displayed excellent cycle stability with 94% capacitance retention even after 5200 charge/discharge cycles entailing excellent recycling durability with repetitive charging/discharging in 5 M KOH electrolyte solution. The carbon nanospheres derived from *Lablab Purpureus* seeds also displayed a peerless Coulombic efficiency of 97%. The insets of Figure 7 shows the 1st and the 5200th cycle of the carbon nanospheres in galvanostatic charging/discharging test and makes it obvious that there is no evident difference between the 1st and the last cycle to clearly indicate the wonderful stability of the carbon nanospheres derived from *Lablab Purpureus* seeds.

Cyclic voltammetry was also repeated between the same potential window of -1 to 0 V, before and after 5200 charge/discharge cycles to investigate the stability of the sample (LP800). The CV curves of LP800 before and after 5200 charge/discharge cycles portray not much deviation (Figure S8). This delineates that there is not much sacrifice in the specific capacitance after 5200 charge/discharge cycles. This excellent behaviour of the electrode can be attributed to the expeditious ion transfer making it a better material for the supercapacitor electrodes.

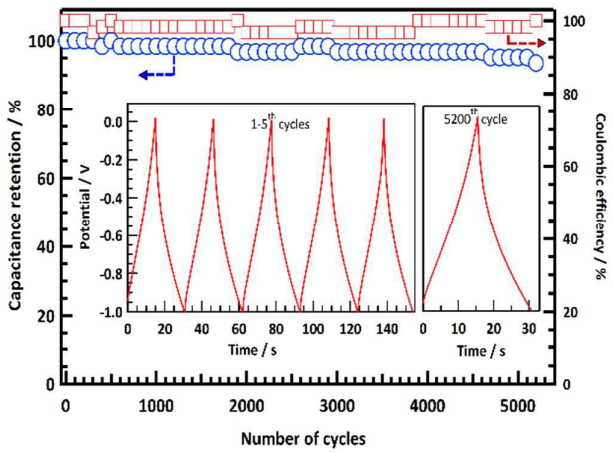

Figure 7 Capacitance retention (left vs. bottom) and Coulombic efficiency (right vs. bottom) of LP800 for 5200 cycles at 3 A g^{-1} (Insets show the charge/discharge of the 1st and 5200th cycles).

DOI: 10.1039/C7DT02392H

3.2.1.4 Electrochemical impedance spectroscopy

EIS of the carbon nanospheres was studied to comprehend the capacitive behaviour, frequency response and to evaluate the charge kinetics of the electrochemical reactions in the fabricated electrode. EIS was performed in the frequency range of 0.10 Hz to 10 kHz (Figure 8). The Nyquist plot of the carbon nanospheres synthesized at 800 ^{o}C (LP800) in different electrolyte concentrations (1.0, 2.5 and 5.0 M KOH) at OCP (Figure 8(a)). The Nyquist plots of the LP800 at different electrolyte concentration shows similar features having a semicircle (insets of Figure 8(a)) in the high frequency range and a vertical linear tail in the low frequency range which can be attributed to the surface impedance existing due to the formation of solid electrolyte interphase, ion transfer resistance and Warburg impedance within the electrode [58]. The equivalent circuit model was used to fit the experimental data and to obtain the EIS parameters. The values of the resistances were found to be very bleak which inferences very high electrical conductivity of the carbon nanospheres derived from *Lablab Purpureus* seeds as listed in Table 2. The straight line in the lower frequency range indicates a pure capacitive behaviour and signifies an ideal supercapacitor [59]. Carbon nanospheres showed a small solution resistance (R_s) and which is decreased with increasing the electrolyte concentration, where it was 1.52 and 0.63 Ω in 1 and 5 M KOH, respectively. On the other hand, charge transfer resistance (R_{ct}) as it was 0.44 and 0.11 Ω in 1 and 5 M KOH, respectively. The EIS results infer that the carbon nanospheres derived from *Lablab Purpureus* seeds have excellent capacitive characteristics. Bode plot denotes the correlation between the phase angle and the frequency response of a system. The bode plot of the carbon nanospheres synthesized at 800 ^{o}C (LP800) in different electrolyte concentrations (1.0, 2.5 and 5.0 M KOH) from which it is evident that the phase angle of the carbon nanospheres in 1.0 and 2.5.0 M KOH electrolyte concentrations have lesser value (-76° and -78°, respectively) in comparison with the phase angle of 5.0 M KOH electrolyte concentration (-80°) which is very near to the phase angle of the ideal capacitor (-90°) inferring that the performance of the carbon nanospheres derived from *Lablab Purpureus* seeds synthesized at 800 ^{o}C in 5.0 M KOH is close to that of an ideal capacitor (Figure 8).

The real (*C'*) and imaginary (*C''*) parts of the capacitance offered by the carbon nanospheres synthesized at 800 ^{o}C (LP800) as a function of frequency at OCP (Figure 8(c) and (d), respectively); which were obtained using the pre–formulated equations [60, 61]. The relaxation time (τ) of the electrode helps in identifying the transition between capacitive and resistive comportment. The frequencies above 1/τ exhibit resistive behaviour and the frequencies below 1/τ exhibit capacitive behaviour. The relaxation time of the electrode was determined to be 0.31 seconds in 5 M KOH. This inherently

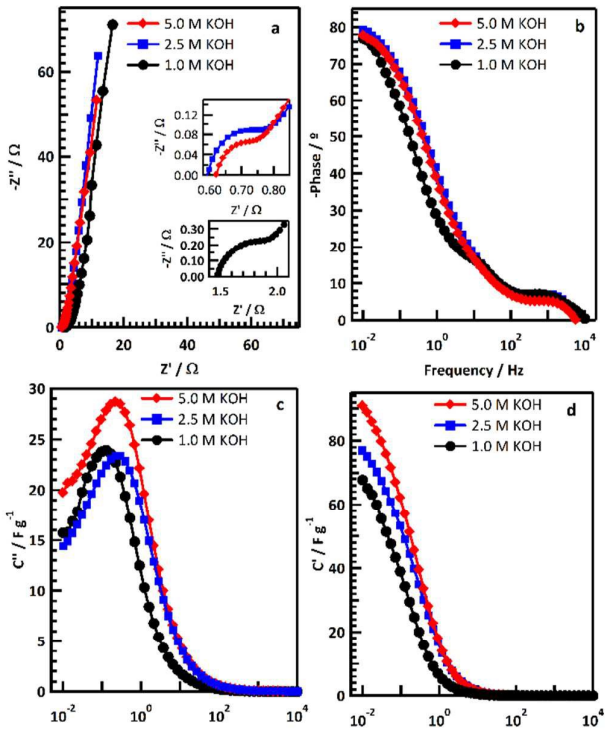

Figure 8: Nyquist (a) and Bode (b) plots (the insets are zoomed view of the plots at high-frequency regions) real (c) and imaginary (d) parts of the capacitance as functions of the frequency at OCP LP800 in different electrolyte concentrations.

stipulates superior electrochemical properties and quick charge/discharge of the electrode fabricated from LP800.

Table 2 Fitting parameters of the experimental impedance data at OCP for carbon nanospheres (LP800) in different electrolyte concentrations.

Electrolyte Concentration	R_s (Ω)	R_{ct} (Ω)	C (mF)	CPE (F)	W (Ω)	τ (s)
1.0 M KOH	1.52	0.44	0.53	0.33	0.19	0.71
2.5 M KOH	0.60	0.16	0.83	0.28	0.34	0.23
5.0 M KOH	0.63	0.11	1.19	0.34	0.39	0.31

Overall, the present study emphasizes the importance of spherical shaped nanoparticles derived from a bio–inspired material; *Lablab Purpureus* seeds in energy storage application. It is worth mentioning that the role of carbon nanospheres helps in incorporating the superior supercapacitor behaviour. Activating the same material might help in enhancing the charging holding capacity and in turn giving rise to an increase in the specific capacitance relatively. Further work in this regard to activate them with various

View Article Online
DOI: 10.1039/C7DT02392H

activating agents is in progress and shall be reported elsewhere.

3.2.2 Practical symmetrical supercapacitor performance

The energy stored in the supercapacitor is directly proportional to the capacitance and the square of voltage, therefore it is imperative to increase the operating voltage of supercapacitors. Generally, the voltage is limited by the stability potential window of the electrolytes [62]. **Error! Reference source not found.**(a), (b) and (c) show CV curves for the symmetrical supercapacitor in the voltage window of 0–1 V, 0–1.4 V at different scan rates and at 25 mV s^{-1} under different potentials windows, respectively. The symmetrical supercapacitor shows the quasi–rectangular CV shapes without redox peaks indicating electrochemical double layer behavior. The wide potential window indicates that this supercapacitor could store higher electrical energy and will be useful in many applications. The operating potential window stability of the symmetric supercapacitor was further tested by galvanostatic charge/discharge. Figure 9(d) shows the charge/discharge curves at 1 A g^{-1} in 5 M KOH in different potential windows ranged from 0–1 to 0–1.7 V. In addition, charge/discharge curves at different current densities in the ranges of 0–1 and 0–1.5 V are shown in Figures 9(e) and (f), respectively. Linear charge and discharge curves with neglected iR drop were obtained, which indicate the supercapacitor has a low internal resistance which leads to better electrochemical double layer performance. It is clearly seen, that supercapacitor shows a wide potential range up to 1.6 V. Specific capacitance was found to be 125 and 103 F g^{-1} under 1.7 V at 0.5 and 1 A g^{-1}, respectively. In addition, the specific capacitance was 129 and 121 F g^{-1} at 0.1 A g^{-1} under 1.5 and 1 V , respectively as shown in **Error! Reference source not found.**(g) and (h), indicating higher charge stored under wider potential.

The energy and power densities can be calculated from CDC data as reported elsewhere [63]. Ragone plot (energy vs. power

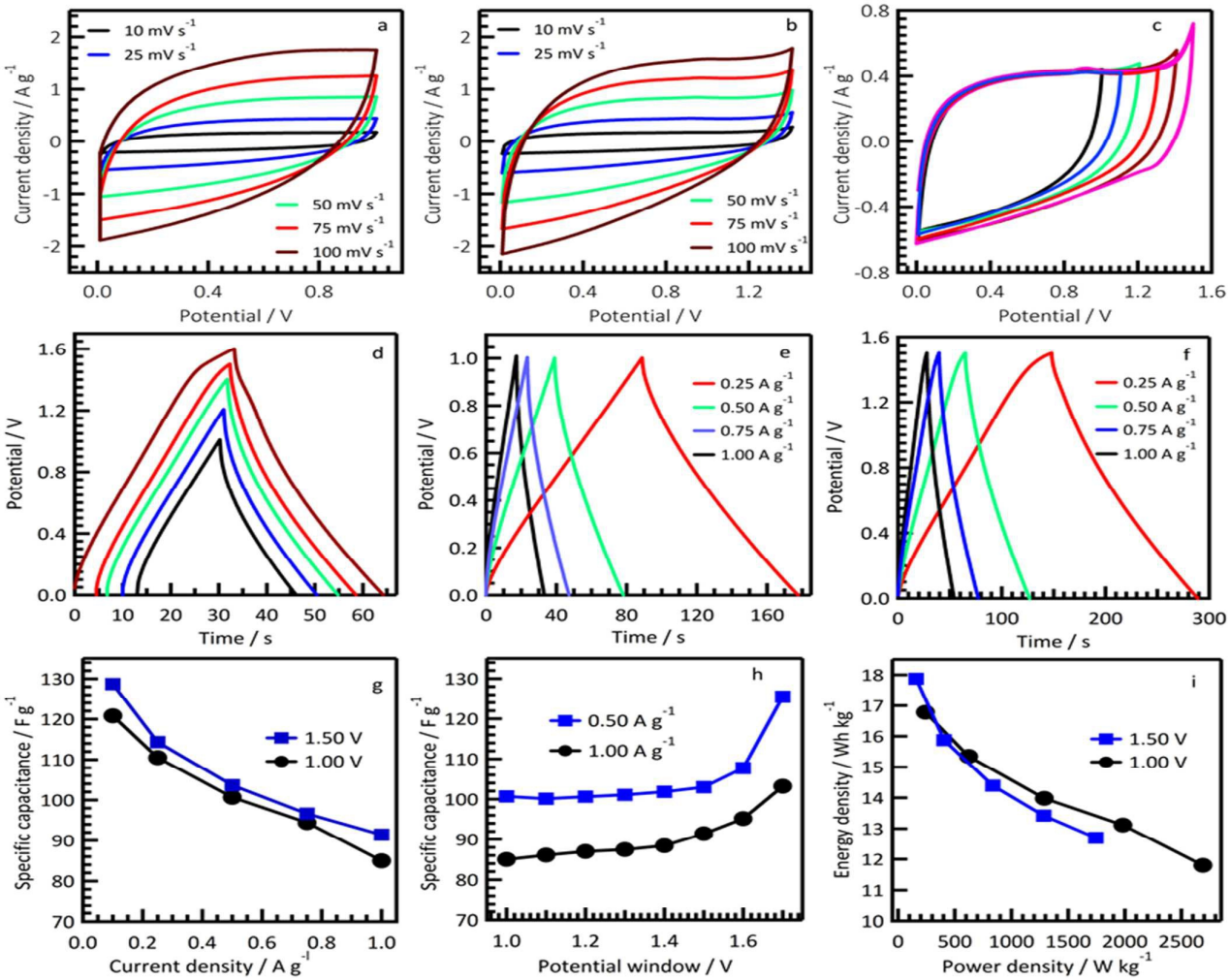

Figure 9 Cyclic voltammetry curves at different scan rates in potential windows of 0-1 V (a),0-1.4 V (b), different potential windows at 25 mV s^{-1} (c), charge-discharge curves at 1 A g^{-1} under different potential windows (d), at different current densities under 1 V (e), 1.5 V (f), specific capacitance as a function of current density (g) and potential window (h) and Ragone plots (i) for LP800 symmetric supercapacitor in 5 M KOH.

View Article Online
DOI: 10.1039/C7DT02392H
Dalton Transactions ARTICLE

density) of the symmetric supercapacitor is shown in **Error! Reference source not found.**(i). The supercapacitor shows a high energy density of 17.9 Wh kg^{-1} under 1.5 V which is higher than it under 1 V. In addition, under the same potential window (1.7 V), the energy values were 17.4 and 14.3 Wh kg^{-1} at 0.5 and 1 A g^{-1}, respectively. This energy density is very close to those obtained for porous nanocarbons from biowaste oil palm leaves precursor (13 W h kg^{-1}) [34] and oil palm empty fruit bunches activated carbon (4.3 W h kg^{-1}) [60].

4. Conclusions

In conclusion, this paper demonstrates a cost effective and environmentally amiable electrode material for energy storage application synthesized from *Lablab Purpureus* seeds by a simple one step pyrolysis technique and its potential application in supercapacitors. It was found that the *Lablab Purpureus* seeds synthesized at 800 ^{o}C showed a specific capacitance of 300 F g^{-1} and remarkable stability even after 5200 cycles. This is attributed to the smaller particle size, due to the high temperature of synthesis. This study indicates that a further increase in specific capacitance is possible if the material is activated.

Acknowledgments

The authors wish to acknowledge Mr. Gadhadar Reddy and his team members, NoPo Nanotechnologies India Pvt Ltd for their help in carrying out Raman spectra. In addition, the authors would like to acknowledge the funding from the Ministry of Education Malaysia in the form of FRGS grant RDU160118 and Universiti Malaysia Pahang grant RDU170357. Moreover, the authors thank the Deanship of Scientific Research at King Khalid University (KKU) for funding this research project Number: (R.G.P.2/2/38).

Notes and references

1. H. D. Abruña, Y. Kiya and J. C. Henderson, *Phys. Today*, 2008, **61**, 43-47.
2. *US Pat.*, 2009.
3. J. B. Goodenough and K.-S. Park, *J. Am. Chem. Soc.*, 2013, **135**, 1167-1176.
4. C. Xu, L. Guo, H. Lu, F. Jiang and P. Yankun, 2016.
5. S. A. Freunberger, *Nat. Energy*, 2016, **1**, 16074.
6. A. Lecocq, G. G. Eshetu, S. Grugeon, N. Martin, S. Laruelle and G. Marlair, *J. Power Sources*, 2016, **316**, 197-206.
7. S. Jogal and K. Sharma, in *CAD/CAM, Robotics and Factories of the Future*, Springer, 2016, pp. 563-568.
8. H. Lim, Y. Shi and Y. Qiao, *Appl. Phys. A*, 2016, **122**, 1-6.
9. P. Thounthong, S. Rael and B. Davat, *J. Power Sources*, 2009, **193**, 376-385.
10. B. E. Conway, *J. Electrochem. Soc.*, 1991, **138**, 1539-1548.
11. A. G. Pandolfo and A. F. Hollenkamp, *J. Power Sources*, 2006, **157**, 11-27.
12. G. A. M. Ali, S. A. Makhlouf, M. M. Yusoff and K. F. Chong, *Rev. Adv. Mater. Sci.*, 2015, **41**, 35-43.
13. P. Sharma and T. Bhatti, *Energy Convers. Manage.*, 2010, **51**, 2901-2912.
14. G. A. M. Ali, E. Y. Lih Teo, E. A. A. Aboelazm, H. Sadegh, A. O. H. Memar, R. Shahryari-Ghoshekandi and K. F. Chong, *Mater. Chem. Phys.*, 2017, **197**, 100-104.
15. Y. Qiu, X. Zhang and S. Yang, *Phys. Chem. Chem. Phys.*, 2011, **13**, 12554-12558.
16. G. A. M. Ali, O. A. Fouad, S. A. Makhlouf, M. M. Yusoff and K. F. Chong, *J. Solid State Electrochem.*, 2014, **18**, 2505-2512.
17. M. M. Yao, Z. H. Hu, Y. F. Liu, P. P. Liu, Z. H. Ai and O. Rudolf, *J. Alloys Compd.*, 2015, **648**, 414-418.
18. G. A. M. Ali, M. M. Yusoff, Y. H. Ng, H. N. Lim and K. F. Chong, *Curr. Appl. Phys.*, 2015, **15**, 1143-1147.
19. G. A. M. Ali, L. L. Tan, R. Jose, M. M. Yusoff and K. F. Chong, *Mater. Res. Bull.*, 2014, **60**, 5-9.
20. G. A. M. Ali, M. M. Yusoff, E. R. Shaaban and K. F. Chong, *Ceram. Int.*, 2017, **43**, 8440–8448.
21. N. Maheswari and G. Muralidharan, *Dalton T*, 2016, **45**, 14352-14362.
22. P. E. Marina, G. A. M. Ali, L. M. See, E. Y. L. Teo, E.-P. Ng and K. F. Chong, *Arabian J. Chem.*, 2016, DOI: 10.1016/j.arabjc.2016.02.006.
23. J. Duay, E. Gillette, R. Liu and S. B. Lee, *Phys. Chem. Chem. Phys.*, 2012, **14**, 3329-3337.
24. S. Nagamuthu, S. Vijayakumar and G. Muralidharan, *Dalton T*, 2014, **43**, 17528-17538.
25. S. Zhang, B. Yin, H. Jiang, F. Qu, A. Umar and X. Wu, *Dalton T*, 2015, **44**, 2409-2415.
26. C. S. Galik, R. C. Abt, G. Latta, A. Méley and J. D. Henderson, *Appl. Energy*, 2016, **172**, 264-274.
27. R. Singh, S. Arora and K. Lal, *Thermochim. Acta*, 1996, **289**, 9-21.
28. G. A. M. Ali, S. A. B. A. Manaf, A. Kumar, K. F. Chong and G. Hegde, *J. Phys. D: Appl. Phys.*, 2014, **47**, 495307–495313.
29. A. Divyashree and G. Hegde, *RSC Adv.*, 2015, **5**, 88339-88352.
30. J. Robertson, *Advances in Physics*, 1986, **35**, 317-374.
31. A. Varzi, A. Balducci and S. Passerini, *J. Electrochem. Soc.*, 2014, **161**, A368-A375.
32. T. Lindström, C. Aulin, M. Gimåker and T. Persson, *IPPTA: Quarterly Journal of Indian Pulp and Paper Technical Association*, 2014, **26**, 53-61.
33. A. Kumar, G. Hegde, S. A. B. A. Manaf, Z. Ngaini and K. Sharma, *Chem. Commun.*, 2014, **50**, 12702-12705.
34. G. A. M. Ali, S. A. A. Manaf, A. Divyashree, K. F. Chong and G. Hegde, *J. Energy Chem.*, 2016, **25**, 734-739.
35. S. Somasundaram, K. Sekar, V. K. Gupta and S. Ganesan, *J. Mol. Liq.*, 2013, **177**, 416-425.
36. M. Kacurakova, P. Capek, V. Sasinkova, N. Wellner and A. Ebringerova, *Carbohydr. Polym.*, 2000, **43**, 195-203.
37. Y. Nishiyama, J. Sugiyama, H. Chanzy and P. Langan, *J. Am. Chem. Soc.*, 2003, **125**, 14300-14306.
38. A. P. Mathew, K. Oksman and M. Sain, *J. Appl. Polym. Sci.*, 2005, **97**, 2014-2025.

View Article Online
DOI: 10.1039/C7DT02392H

39. A. Divyashree, S. A. B. A. Manaf, S. Yallappa, K. Chaitra, N. Kathyayini and G. Hegde, *J. Energy Chem.*, 2016, **25**, 880-887.
40. Z.-G. Shi, Y.-Q. Feng, L. Xu, S.-L. Da and M. Zhang, *Carbon*, 2004, **42**, 1677-1682.
41. Z. Li, D. Wu, Y. Liang, F. Xu and R. Fu, *Nanoscale*, 2013, **5**, 10824-10828.
42. B. S. Girgis, Y. M. Temerk, M. M. Gadelrab and I. D. Abdullah, *Carbon Lett.*, 2007, **8**, 95-100.
43. A. N. Mohan and B. Manoj, *Int. J. Electrochem. Sci.*, 2012, **7**, 9537-9549.
44. Y. Wang, D. C. Alsmeyer and R. L. McCreery, *Chem. Mater.*, 1990, **2**, 557-563.45. L. Bokobza, J.-L. Bruneel and M. Couzi, *C J. Carbon Res.*, 2015, **1**, 77-94.
46. M. Matthews, M. Pimenta, G. Dresselhaus, M. Dresselhaus and M. Endo, *Phys. Rev. B*, 1999, **59**, R6585.
47. C. Zheng, X. Zhou, H. Cao, G. Wang and Z. Liu, *J. Power Sources*, 2014, **258**, 290-296.
48. J. N. Lekitima, K. I. Ozoemena, C. J. Jafta, N. Kobayashi, Y. Song, D. Tong, S. Chen and M. Oyama, *J. Mater. Chem., A*, 2013, **1**, 2821-2826.
49. J. Gomez and E. E. Kalu, *J. Power Sources*, 2013, **230**, 218-224.
50. V. Subramanian, C. Luo, A. Stephan, K. Nahm, S. Thomas and B. Wei, *J. Phys. Chem. C*, 2007, **111**, 7527-7531.
51. J. Ma, T. Xue and X. Qin, *Electrochim. Acta*, 2014, **115**, 566-572.
52. G. Lota, T. A. Centeno, E. Frackowiak and F. Stoeckli, *Electrochim. Acta*, 2008, **53**, 2210-2216.
53. D. Hulicova, J. Yamashita, Y. Soneda, H. Hatori and M. Kodama, *Chem. Mater.*, 2005, **17**, 1241-1247.
54. A. Elmouwahidi, Z. Zapata-Benabithe, F. Carrasco-Marín and C. Moreno-Castilla, *Bioresour. Technol.*, 2012, **111**, 185-190.
55. M. Balathanigaimani, W.-G. Shim, M.-J. Lee, C. Kim, J.-W. Lee and H. Moon, *Electrochem. Commun.*, 2008, **10**, 868-871.
56. G. A. M. Ali, M. M. Yusoff and K. F. Chong, *ARPN J. Eng. Appl. Sci.*, 2016, **11**, 9712 -9717.
57. J. Zhang, L. Gong, K. Sun, J. Jiang and X. Zhang, *J. Solid State Electrochem.*, 2012, **16**, 2179-2186.
58. S. Yang, X. Feng and K. Müllen, *Adv. Mater.*, 2011, **23**, 3575-3579.
59. Y. Yoon, K. Lee, C. Baik, H. Yoo, M. Min, Y. Park, S. M. Lee and H. Lee, *Adv. Mater.*, 2013, **25**, 4437-4444.
60. R. Farma, M. Deraman, A. Awitdrus, I. Talib, E. Taer, N. Basri, J. Manjunatha, M. Ishak, B. Dollah and S. Hashmi, *Bioresour. Technol.*, 2013, **132**, 254-261.
61. C. Portet, P. L. Taberna, P. Simon, E. Flahaut and C. Laberty-Robert, *Electrochim. Acta*, 2005, **50**, 4174-4181.
62. L. L. Zhang and X. Zhao, *Chem. Soc. Rev.*, 2009, **38**, 2520-2531.
63. S. Deng, D. Sun, C. Wu, H. Wang, J. Liu, Y. Sun and H. Yan, *Electrochim. Acta*, 2013, **111**, 707–712.

View Article Online
DOI: 10.1039/C7DT02392H

Carbon nanospheres derived from Lablab Purpureus as a high performance supercapacitor electrode: Green approach

Gomaa A. M. Ali, Divyashree A, Supriya S, Kwok Feng Chong, Anita S. Ethiraj, M V Reddy, H. Algarni and Gurumurthy Hegde

Graphical Abstract:

Carbon nanospheres prepared from Lablab Purpureus using a green approach showed high capacitance (300 F g^{-1}) and stability (94%)